Epitaxial Growth of Sexiphenyl on Al(111): From Monolayer to Crystalline Films

ARTICLE *in* LANGMUIR · AUGUST 2004

Impact Factor: 4.46 · DOI: 10.1021/la049529q · Source: PubMed

6 AUTHORS, INCLUDING:

Ján Ivančo
Slovak Academy of Sciences
55 PUBLICATIONS **672** CITATIONS
SEE PROFILE

Michael G Ramsey
Karl-Franzens-Universität Graz
192 PUBLICATIONS **4,172** CITATIONS
SEE PROFILE

Ingo Salzmann
Humboldt-Universität zu Berlin
82 PUBLICATIONS **1,929** CITATIONS
SEE PROFILE

Roland Resel
Graz University of Technology
269 PUBLICATIONS **3,753** CITATIONS
SEE PROFILE

Epitaxial Growth of Sexiphenyl on Al(111): From Monolayer to Crystalline Films

Barbara Winter, Jan Ivanco, Falko P. Netzer, and Michael G. Ramsey*

Institute of Experimental Physics, Karl Franzens University Graz, Universitätsplatz 5, A-8010 Graz, Austria

Ingo Salzmann and Roland Resel

Institute of Solid State Physics, Graz University of Technology, Petersgasse 16, A-8010 Graz, Austria

Received February 23, 2004. In Final Form: May 26, 2004

A combination of in situ surface sensitive-techniques, UV photoemission and low energy electron diffraction, with ex situ bulk sensitive X-ray diffraction reveals the formation of epitaxial thin films of sexiphenyl on Al(111) starting from the first monolayer. For room temperature growth, highly ordered films are formed with a unique alignment of the sexiphenyl molecules with the long axes of all molecules aligned parallel to both the surface and the ⟨110⟩ azimuthal directions of Al(111). This is related to a densely packed highly commensurate first monolayer, which acts as a template for the unique (21$\bar{3}$) crystallite orientation observed.

Introduction

For organic devices, the interface of the active organic films with the inorganic substrates is decisive to their function. On one hand, the nature of the interface is crucial to the charge injection into the film. It can, on the other hand, also influence the growth, morphology, and structure of the film critical for charge transport within the film. The orientation and structure of the first molecular monolayer is recognized to be decisive to the subsequent crystalline structure of thin films and has, thus, stimulated investigations into monolayer structures of large organic molecules.[1−3] However, few studies have bridged the gap from the first monolayer to films of device relevant thicknesses.

Among the organic semiconductors, the aromatic molecule sexiphenyl (6P, $C_{36}H_{26}$) plays an outstanding role because of the highly efficient light emission in the blue-visible range and the strong tendency to crystallize. As an active device material, 6P has been successfully used in a number of electronic and optoelectronic applications such as light-emitting devices, solar cells, and field effect transistors.[4−6] Aluminum is commonly used as the metallic electrode with the device performance being highly dependent on the details of the interface between 6P and the aluminum.[7−9] Important roles are also played by the molecular alignment of 6P relative to the electrodes[10] and the size of the single crystalline domains.[11] Numerous X-ray diffraction (XRD) studies can be found in the literature of 6P films grown on various substrates;[12−14] in these studies the films were generally relatively thick (∼200 nm) and consisted of a number of different crystallite orientations. Moreover, the azimuthal orientation of such films is generally not good displaying in their pole figures at best crescents (e.g., 6P on mica).[14] Here, we present results of a study of the structure of 6P grown on Al(111) which is unique in that a highly crystalline, single-phase film is obtained where all the molecules are not only oriented parallel to the substrate surface but are also aligned along the principle azimuthal directions of the substrate surface. This unique film orientation and epitaxy is here related to the highly ordered first molecular monolayer on which it grows.

Experimental Section

Thin films of 6P on Al(111) were prepared under ultrahigh vacuum conditions (base pressure 1×10^{-10} mbar) in an angle-resolving ultraviolet photoemission spectrometer (ARUPS) system. Prior to the deposition process, the Al(111) single-crystal surface was cleaned by Ar^+-sputtering and subsequently annealed at 700 K. The purity and order of the surface was checked by means of UV photoemission and low energy electron diffraction (LEED). 6P, purchased from Tokyo Chemical Industries, was thoroughly degassed in situ and evaporated from a Knudsen cell onto the substrate whose temperature was monitored by a thermocouple attached to it. The deposition was controlled by a quartz microbalance; deposition rates of 0.2 nm/min were used,

(1) England, C. D.; Collins, G. E.; Schuerlein, T. J.; Armstrong, N. R. *Langmuir* **1994**, *10*, 2748.
(2) France, C. B.; Schroeder, P. G.; Forsythe, J. C.; Parkinson, B. A. *Langmuir* **2003**, *19*, 1274.
(3) Chen, Q.; McDowall, A. J.; Richardson, N. V. *Langmuir* **2003**, *19*, 10164.
(4) Tasch, S.; Brandstaetter, C.; Meghdadi, F.; Leising, G.; Froyer, G.; Athouel, L. *Adv. Mater.* **1997**, *9*, 33.
(5) Meinhardt, G.; Graupner, W.; Feistritzer, G.; Schröder, R.; List, E. J. W.; Pogantsch, A.; Dicker, G.; Schlicke, B.; Schulte, N.; Schlüter, A. D.; Winter, G.; Hanack, M.; Scherf, U.; Müllen, K.; Leising, G. *Proc. SPIE-Int. Soc. Opt. Eng.* **1999**, *46*, 3623.
(6) Gundlach, D. J.; Lin, Y.-Y.; Jackson, T. N.; Schlom, D. G. *Appl. Phys. Lett.* **1997**, *71*, 853.
(7) Koch, N.; Yu, L. M.; Parente, V.; Lazzaroni, R.; Johnson, R. L.; Leising, G.; Piiraux, J. J.; Bredas, J. L. *Adv. Mater.* **1998**, *10*, 1038.
(8) Koch, N.; Pongantsch, A.; List, E. J. W.; Blyth, R. I. R.; Ramsey, M. G.; Netzer, F. P.; Leising, G. *Appl. Phys. Lett.* **1999**, *74*, 2909.
(9) Ivanco, J.; Winter, B.; Netzer, F. P.; Ramsey, M. G. *Adv. Mater.* **2003**, *15*, 1812.
(10) Yanagi, H.; Okamoto, S. *Appl. Phys. Lett.* **1997**, *71*, 2563.
(11) Brandt, H.-J.; Resel, R.; Keckes, J.; Koppelhuber-Bitschnau, B.; Koch, N.; Leising, G. *Mater. Res. Soc. Symp. Proc.* **1999**, *561*, 161.
(12) Smilgies, D.-M.; Boudet, N.; Yanagi, H. *Appl. Surf. Sci.* **2002**, *189*, 24.
(13) Plank, H.; Resel, R.; Sariciftci, N. S.; Andreev, A.; Sitter, H.; Hlawacek, G.; Teichert, C.; Thierry, A.; Lotz, B. *Thin Solid Films* **2003**, *443*, 108. Resel, R. *Thin Solid Films* **2003**, *433*, 1.
(14) Plank, H.; Resel, R.; Andreev, A.; Sariciftci, N. S.; Sitter, H. *J. Cryst. Growth* **2002**, *237−239*, 2076.

10.1021/la049529q CCC: $27.50
Published on Web 07/29/2004

and the nominal film thicknesses quoted are derived from the accepted density of 6P of 1.3 g/cm^3. LEED was performed with a standard front-view LEED optics for a variety of primary energies. The high electron beam currents (~1 μA) quickly destroyed the molecular order. All images were, therefore, obtained while manually rastering the sample, and for each image, a new substrate and film preparation were required. LEED simulations of surface structures were performed with the Sarch-Latuse program. Prior to removal for the ex situ XRD investigations, the samples where characterized by angle-resolved ultraviolet photoemission spectroscopy (UPS) and work function (ϕ) measurements obtained from the secondary electron cutoff.

Ex situ XRD studies were performed on the in situ characterized films with a Philips X'Pert System equipped with an ATC3 texture cradle using Cr Kα radiation. Monochromatization was obtained by a flat crystal of graphite; Cr Kα as well as higher harmonics of this radiation could pass. Specular scans, pole figures, and Θ/2 Θ scans were performed simultaneously on the Al(111) single-crystal substrate and on the 6P layer to obtain the crystallographic properties of both the substrate and the molecular film and their mutual relationship. Evaluation of the diffraction data was performed on the basis of the single-crystal structure of aluminum (a = 2.864 Å) and 6P (a = 8.091 Å, b = 5.565 Å, c = 26.24 Å, and β = 98.18°).[15,16]

Results and Discussion

The growth of 6P on Al(111) has been followed by angle-resolved photoemission of the valence band and work function measurements from submonolayer coverages up to 30-nm nominal thickness for substrate temperatures of 80 K (liquid nitrogen temperature), 300 K (room temperature, RT), and 400 K (HT). Figure 1a,b displays the development of the valence band spectra and work function as a function of increasing 6P exposure at RT. Irrespective of substrate temperature, the work function behavior with increasing coverages was identical with a rapid decrease of ϕ from 4.25 to 3.75 eV occurring in the first 4 Å of exposure and remaining constant beyond this coverage for exposures up to 300 Å. The spread of ϕ values for various thicker films (15−300 Å) is indicated by the bar in Figure 1b. The work function changes are due to the interface dipole arising from the interaction of the molecules in the first molecular layer with the substrate, and 4 Å is, thus, considered as the completion of the first monolayer.

The valence band emission features grow rapidly in intensity in the first 4 Å of exposure and are saturated by around 20 Å for room-temperature growth. By this exposure, the Fermi level step of the substrate is no longer visible. This behavior is similar to growth at 80 K, where molecular mobility will be low, and is indicative of layer-by-layer growth. In contrast, for growth at elevated temperatures, although the behavior up to 4 Å is identical, beyond this monolayer the spectral form changes and the Fermi level remains visible up to ~100 Å exposure, indicating island growth.

The valence band spectrum of 6P (see Figure 1a) is reasonably well understood; the deeper lying bands (B−D) are associated primarily with intra-ring orbitals and are very similar to those of benzene. Band A, the π band, consists of 12 orbitals developing from the inter-ring bonding and antibonding combinations of the two degenerate e_{1g} orbitals of benzene.[17,18] The valence band spectra

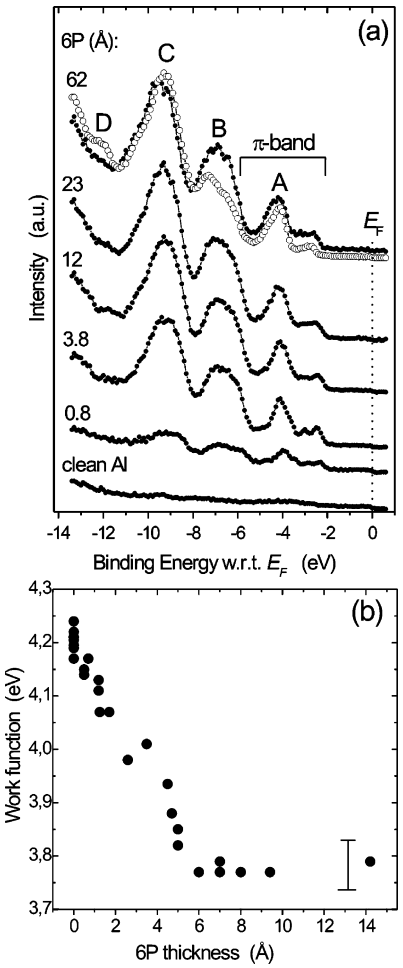

Figure 1. (a) Typical UPS spectral series for 6P growth on Al(111) at RT using unpolarized HeI excitation with an electron emission angle, Θ, of 50°. The normal emission spectra for 62 Å is also shown (open circles). (b) Work function as a function of 6P exposure; the bar indicates the range of values obtained for various thick film preparations on clean Al(111).

in the coverage regime up to a monolayer is very distinct and displays strong angular effects as illustrated in Figure 2, where the spectral series as a function of electron emission angle for 3.8 Å of 6P is displayed.

Band D, associated with the σ_{C-H} orbitals, is only prominent in normal emission; bands B and C appear to shift in energy as a result of changes in relative emission intensity from the orbitals within them. The angular effects are particularly pronounced for the highest occupied molecular orbital emissions, HOMO and HOMO-1, which have no intensity in normal emission but become prominent at higher emission angles. Such strong ARUPS effects are indicative of a homogeneous highly oriented molecular species at the surface.[19] The angular behavior remains, although it becomes less pronounced, for multilayer films grown at RT (e.g., see Figure 1a for 62 Å), suggesting that the orientation of the molecules in the monolayer is retained for RT-grown multilayers. For RT growth beyond the monolayer, there are no shifts, neither rigid nor relative to each other, in the energy of the orbital emissions. The lack of differential shifts indicates that no particular orbitals are strongly involved in the bond to the surface. This behavior is similar to that of benzene on

(15) Figgins, B. F.; Jones, G. O.; Riley, D. P. *Philos. Mag.* **1956**, *1*, 747.
(16) Baker, K. N.; Fratini, A. V.; Resch, T.; Knachel, H. C.; Adams, W. W.; Socci, E. P.; Farmer, B. L. *Polymer* **1993**, *34*, 1571.
(17) Seki, K.; Karlsson, U. O.; Engelhardt, R.; Koch, E.-E.; Schmidt, W. *Chem. Phys.* **1984**, *91*, 459.
(18) Ramsey, M. G.; Steinmüller, D.; Schatzmayr, M.; Kiskinova, M.; Netzer, F. P. *Chem. Phys.* **1993**, *177*, 349.
(19) Netzer, F. P.; Ramsey, M. G. *Crit. Rev. Solid State Mater. Sci.* **1992**, *17*, 397.

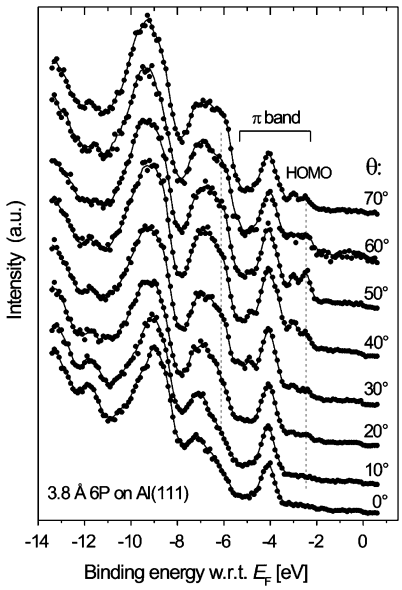

Figure 2. UPS valence band spectra of the 6P monolayer (3.8 Å) as a function of electron emission angle, Θ.

Al(111) where an electrostatic bond was concluded[20] and is different to that of 6P on Ni(110) where the π orbitals where shifted to higher binding energies relative to the σ orbitals due to π bonding with the substrate.[18] The lack of a rigid shift in going from monolayer to multilayer is also similar to benzene on Al(111) and indicates that the screening of the photohole in the monolayer from the electrons of the metallic substrate is only as effective as that due to intermolecular screening in the multilayer film. This again suggests a weak bond to the Al surface with the molecule positioned relatively high above the surface. That the molecule−surface interactions are only slightly stronger than the molecule−molecule interactions is also attested by the fact that the monolayer molecules desorb at 530 K, only 40 K above the multilayer desorption temperature.

The valence band spectra of 6P films grown at elevated temperature on clean Al(111) or at RT on oxidized Al(111) are distinctly different to those of films grown at RT on clean Al(111).[9] The difference is manifested in the energy spread and line shape of the π band and, more objectively, in their HOMO binding energies with respect to the vacuum level of 5.8 and 6.4 eV, respectively. This difference in ionization potentials has been argued to be due to 6P in the films being either in planar or in twisted conformations, respectively.[9] The ionization potential of the molecules in the first monolayer of 6.4 eV, the same as for multilayers grown at RT, thus, suggests that the aromatic rings in the monolayer molecules are not coplanar.

The monolayer of 6P whether grown at RT or HT or created by desorbing the multilayer shows the same ARUPS behavior and long-range order in LEED. Figure 3a displays the LEED pattern from 3.8-Å 6P at a primary energy of 42 eV. Here, the outermost points on the edge of the image (indicated by circles) are at the position of the hexagon of first-order reflexes of the Al(111) surface.

The relatively poor definition in the 6P electron diffraction pattern is not necessarily due to poor order but rather reflects the sensitivity of the monolayer to the electron beam. The patterns clearly reflected the threefold symmetry of the Al(111) substrate and are characterized by relatively well-defined points radiating along the

(20) Duschek, R.; Mittendorfer, F.; Blyth, R. I. R.; Netzer, F. P.; Hafner, J.; Ramsey, M. G. *Chem. Phys. Lett.* **2000**, *348*, 43.

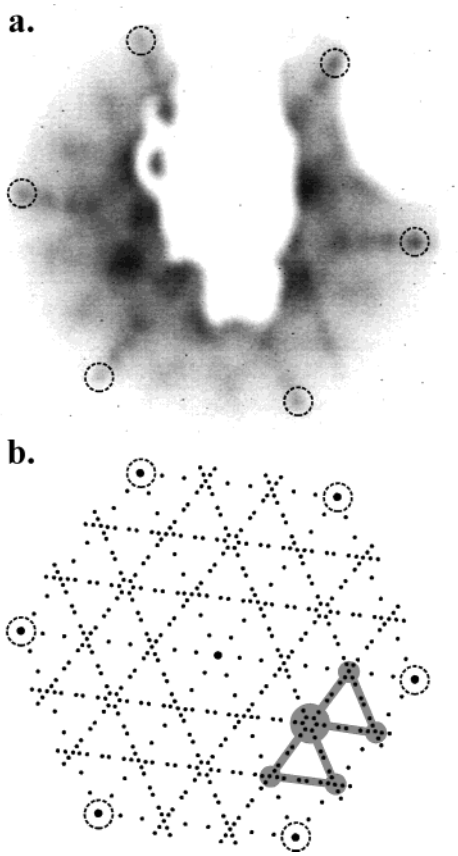

Figure 3. (a) LEED pattern of 3.8 Å of 6P on Al(111) for a primary electron energy of 42 eV. (b) LEED simulation for the proposed $\begin{pmatrix} 9 & 1 \\ 0 & 3 \end{pmatrix}$ 6P overlayer. The encircled points indicate the positions of the Al(111) integral order reflexes, while shading indicates that smearing the would arise from closely spaced points.

principle azimuthal directions with a spacing of $^1/_9$ of the Al *k*-space vector. In the regions between the principle azimuths, diffuse triangles can be discerned with side lengths $^1/_3$ of that of the Al *k*-space vector. This suggests that the 6P overlayer is related to a simple (9 × 3) overlayer structure, that is, a 2-dimensional lattice unit cell of 25.7 × 8.6 Å with an angle of 60°. This commensurate structure, however, cannot explain why the spots along the principle azimuths are defined while the triangles are diffuse. This could be a result of incommensurability in the short real-space direction, such as (9 × 3.1), or a degree of disorder in this direction. Unlike the common case for LEED of overlayer structures, the two-dimensional unit cell here cannot be simply obtained by observation without gross assumptions such as the angle between the overlayer unit cell vectors. Numerous LEED simulations were performed with the result that the unit cell dimensions were concluded to be in the range 25 (±2) × 8 (±1) Å depending on the angle assumed between them. The long dimension is in the range of the molecular length and suggests that the molecules lie near parallel to the surface in agreement with the amount of material required to form the monolayer. It should be noted that simulations of none of the planes of the known bulk 6P crystal structure[16] in any way approximated the observed LEED pattern.

Ex situ XRD investigations were performed on films with nominal thicknesses of 30 nm grown at RT and HT. Despite expectations that elevated temperature growth would improve order, the HT-grown films displayed very

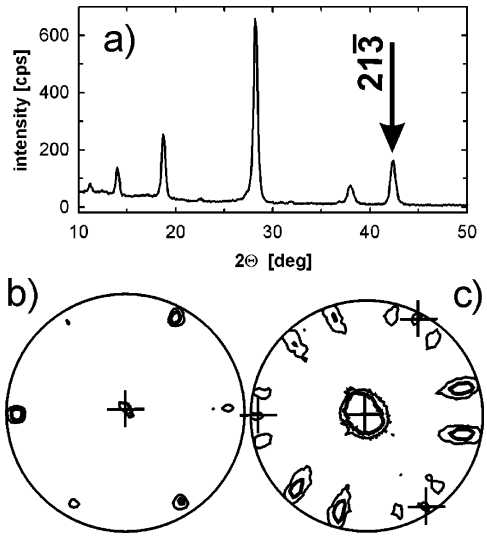

Figure 4. XRD studies of a 30-nm-thick film of 6P grown on Al(111) at RT. (a) A specular scan with the $21\bar{3}$ reflection of 6P indicated. (b and c) Pole figures of the $20\bar{3}$ and the $11\bar{1}$ reflections. The limits of representation are 40 and 25°, respectively. Elevated and high pole densities are denoted by thin and thick contour lines, respectively, and the crosses mark scattering from the Al substrate.

poor order[21] while those grown at RT showed a high degree of order despite their thinness. A specular scan of the film grown at RT is displayed in Figure 4a. Higher harmonic reflections from the aluminum substrate and an additional single reflection of 6P are observed. This reflection from the molecular film is as well-defined as those of the single-crystal substrate. The position of the 6P peak at 42.38° agrees well with the calculated peak position for the $(21\bar{3})$ orientation of 6P of 42.40°. Pole figures on the $21\bar{3}$, $20\bar{3}$, and $11\bar{1}$ reflections of 6P were taken; the results for the $20\bar{3}$ and $11\bar{1}$ ones are shown in Figure 4b,c, respectively. The pole figures are represented by stereographic projections, and directions of enhanced pole densities (EPDs) are marked by thin and thick contour lines for elevated and high pole densities, respectively. As a result of the scattering of higher harmonics on aluminum, some additional EPDs due to the substrate appear in the pole figures of 6P; they are marked by crosses within the pole figures. The combination of substrate and film features graphically illustrates the epitaxy of the 6P film. In comparison to the results of XRD investigations on 6P films grown on other substrates, the presented thin films grown at RT on Al(111) display a very high degree of order and epitaxy. On the scale of the specular scan of Figure 4a, the equivalent scan for the 30-nm HT-grown films shows effectively no 6P-related features. Close inspection of specular scans from such films reveal extremely weak reflections due to both (001) and $(21\bar{3})$ orientations while pole plots show no detectable 6P features.

Comparing the calculated spherical projection of a single 6P crystal with the observed EPDs of Figure 4, the following conclusions can be made for RT-grown films on Al(111): (i) 6P crystallizes in a single phase; (ii) only one orientation of the 6P crystallites parallel to the Al(111) surface is observed, namely, $(111)_{Al} \| (21\bar{3})_{6P}$; and (iii) there is high alignment of the 6P crystallites relative to particular directions at the Al(111) substrate. With this result and given the arrangement of the molecules within the crystallographic unit cell, the orientation of the molecules relative to the Al(111) single crystal is determined to be parallel to the surface with the long axes of all molecules aligned along the $\langle 1\bar{1}0 \rangle$ azimuth of Al(111). Starting from an aligned molecule, four rhomboidal $(21\bar{3})$ oriented crystallites are possible, and this, in combination with the threefold symmetry of the substrate, leads to the 12 symmetry equivalent crystallite alignments observed (see Figure 4c).

Although XRD probes only the bulk properties, it is obvious that the observed unique molecular orientation should be also present within the first monolayer. In combination with the observed surface unit cell of a single monolayer from LEED, the molecular arrangement at the Al(111) interface can be deduced. Figure 5a shows the projection of a $(21\bar{3})$ 6P plane on the Al(111) substrate with its two-dimensional unit cell, 13.76 × 26.92 Å with an angle of 85.87°. The molecules have been drawn to scale and are oriented along the $[1\bar{1}0]$ azimuth as determined from the XRD results.

The $(21\bar{3})$ plane can in no way account for the observed LEED pattern, irrespective of the orientation of the 6P unit cell, because its area is of the order of twice the size of that suggested by the LEED. The van der Waals size of the molecule is indicated in Figure 5, and clearly a $(21\bar{3})$ plane leaves a large Al area free for the adsorption of additional molecules. A simple commensurate (9 × 3) overlayer structure suggested by the LEED (see previous) can be constructed simply from the $(21\bar{3})$ plane by doubling the number of molecules in the plane and moving them slightly such that each molecule has the same adsorption site. Support for a first monolayer with double the density of a single $(21\bar{3})$ plane comes also from the quantity of material required to saturate the first layer. Given the nominal density of 6P of 1.3 g/cm^3, the "thickness" for a single $(21\bar{3})$ plane would be only 1.58 Å, slightly less than half the microbalance measurement for the saturation of the first layer of 3.8 ± 0.5 Å. The van der Waals radius allows the molecules to fit side-by-side easily in a (9 × 3) structure, and the molecules can be offset to minimize van der Waals overlap at their ends, as illustrated in Figure 5b. Although the ARUPS suggests the molecules in the monolayer are not planar, for simplicity, the molecules have been drawn as planar, thus, exaggerating the intermolecular overlap. It is also worth noting at this point that in general bonding to surfaces can lead to structures much denser than their van der Waals radii would otherwise allow.[19] The LEED simulation of this "modified 9 × 3" structure, precisely designated in the matrix notation as $\begin{pmatrix} 9 & 1 \\ 0 & 3 \end{pmatrix}$, is in good agreement with the observed LEED pattern in that it displays the distinct, regularly spaced reflexes along the principle azimuthal directions while between them irregularly spaced points can explain the diffuse triangles observed (see Figure 3b) without invoking disorder. Within this model, all molecules occupy equivalent sites; however, the registry to the substrate is a priori unknown. The dimensions of the molecule are such that a degree of commensurability for the individual rings of the molecules is also possible. The inter-ring distance is 4.27 Å,[16] which is very close to 1.5 times the lattice constant of Al (4.296 Å); thus, if the molecules were placed on top of the close-packed Al rows the rings would occupy alternating on-top, bridge sites with the ends of the molecules being different. For benzene on Al(111), the hollow site has been calculated to be slightly more favorable than bridge or on-top sites.[20] Consequently, the 6P molecules have been placed in hollow sites in the figure. Interestingly, the dimensions of the molecule are such that each ring of the molecules occupies near

(21) Resel, R.; Salzmann, I.; Hlawacek, G.; Teichert, C.; Koppelhuber, B.; Winter, B.; Krenn, J.; Ivanco, J.; Ramsey, M. G. *Organic Electronics* **2004**, *5*, 45.

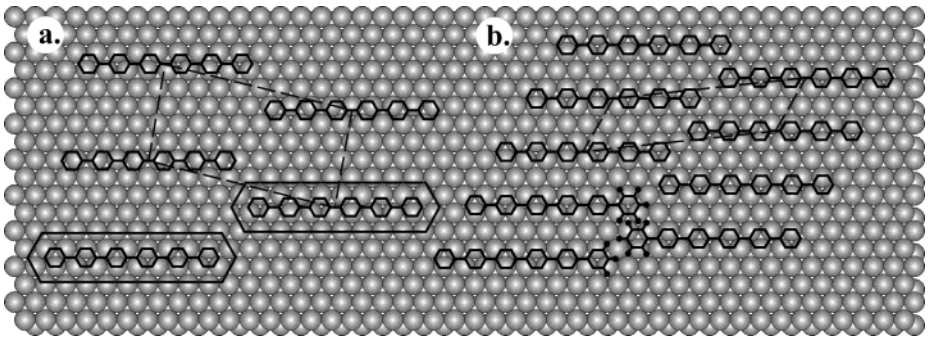

Figure 5. (a) Projection of a $(21\bar{3})$ plane of 6P onto the Al(111) surface with the two-dimensional unit cell (26.92 Å × 13.76 Å, $\beta = 94.13°$) and the van der Waals size indicated. (b) The proposed $\begin{pmatrix} 9 & 1 \\ 0 & 3 \end{pmatrix}$ 6P monolayer (27.32 Å × 8.59 Å, $\beta = 54.79°$).

equivalent hollow sites (the rings occupy alternating face-centered cubic and hexagonal close-packed hollow sites on the surface). Commensurate structures are generally energetically favorable,[1,22] and the structure proposed here, with both the molecules and the rings within the molecules all occupying equivalent sites, is thus likely. Recent low-temperature scanning tunneling microscopy results of Hla et al.[23] for isolated 6P adsorbed on Ag(111) lend support to the proposed adsorption site. On Ag, which has a similar lattice constant to Al, the molecules were observed to be oriented along the $[1\bar{1}0]$ azimuth in the all-hollow sites, moreover, the molecules appeared non-planar in agreement with the reduced conjugation inferred from the ionization potential here.

There are few examples reported in the literature of epitaxial growth of 6P films on inorganic substrates. XRD studies on thin films grown on KCl(100) reveal several epitaxial orientations with the coexistence of molecules oriented both perpendicular and parallel to the surface [i.e., (001) and $(20\bar{3})$ orientations].[12] The epitaxial order within films grown on mica (001) is also defined by multiple orientations where the molecules are near parallel to the surface [$(11\bar{1})$ and $(11\bar{2})$].[13] In all these cases, cleavage planes of 6P crystallites (crystallographic planes with dense-packed molecules) are found. However, the unique $(21\bar{3})$ molecular orientation of this work with the molecules parallel to the substrate surface has not been observed until now. The occurrence of epitaxial growth in molecular thin films is connected with a fine balance between the intermolecular interactions and the interaction of the molecules to the substrate.[1−3,22,24] In the present case, the enhanced electrostatic interaction of the molecules with the metal substrate together with a lattice match which allows a dense, highly commensurate structure, where not only each molecule but also each ring in each molecule can occupy equivalent sites, leads to the molecules in the first layer having a specific azimuthal orientation ($\langle 1\bar{1}0 \rangle$). The growth on this monolayer lattice to a bulk 6P structure with the unique $(21\bar{3})$ orientation requires relatively little molecular rearrangement, and the former can be viewed as a good template for the latter.

Acknowledgment. This work was supported by the Austrian Science Foundation (FWF).

LA049529Q

(22) Hooks, D. E.; Fritz, T.; Ward, M. D. *Adv. Mater.* **2001**, *13*, 227.
(23) Hla, S.-W. Private communication.
(24) Umbach, E.; Scholowski, M.; Fink, R. *Appl. Phys. A* **1996**, *63*, 565.